

Direct spectroscopic evidence for ionized PAHs in the interstellar medium

G.C. Sloan^{1 2}

T.L. Hayward³

L.J. Allamandola²

J.D. Bregman²

B. DeVito³

D.M. Hudgins²

¹School of Physics, University College, Australian Defence Force Academy, Canberra, ACT
2600, Australia

²NASA Ames Research Center, MS 245-6, Moffett Field, CA 94035-1000

³Center for Radiophysics and Space Research, Cornell University, Ithaca, NY 14853

Received _____; accepted _____

ABSTRACT

Long-slit 8–13 μm spectroscopy of the nebula around NGC 1333 SVS 3 reveals spatial variations in the strength and shape of emission features which are probably produced by polycyclic aromatic hydrocarbons (PAHs). Close to SVS 3, the 11.2 μm feature develops an excess at $\sim 10.8\text{--}11.0$ μm , and a feature appears at ~ 10 μm . These features disappear with increasing distance from the central source, and they show striking similarities to recent laboratory data of PAH cations, providing the first identification of emission features arising specifically from ionized PAHs in the interstellar medium.

Subject headings: (ISM:) dust, extinction; ISM: molecules; infrared: ISM: lines and bands

1. Introduction

Gillett, Forrest, & Merrill (1973), in a spectroscopic study of planetary nebulae, discovered a series of unidentified infrared (UIR) bands, now known to include features at 3.3, 6.2, 7.7, 8.6, and 12.7 μm . Since then the UIR bands have been observed in a rich variety of astronomical sources (see Allamandola 1996 for a recent review). Polycyclic aromatic hydrocarbons (PAHs) were first introduced as a possible carrier of the UIR bands by Leger & Puget (1984) and Allamandola, Tielens, & Barker (1985). While other carriers have been proposed for the UIR bands, none have proven as successful as the PAH model in explaining the observed spectral details. Nonetheless, many differences exist between earlier laboratory and astronomical spectra, including the relative strength of the features and the wavelengths at which they appear, and these differences have prevented the PAH model from gaining wider adherence.

A major discrepancy exists between the relative intensities of the features in the 10–13 μm region (C–H out-of-plane bending modes) and the features in the 6–9 μm region (C–C modes and the C–H in-plane bend at 8.6 μm). In laboratory spectra of neutral PAHs, the C–C modes are much weaker than the features at longer wavelengths, but in astronomical spectra, the C–C modes are stronger. Allamandola et al. (1985) originally suggested that most or all PAHs in the interstellar medium would be ionized, due to their low ionization potential (~ 6 eV), and laboratory investigations of PAH cations show better agreement with the observed UIR spectra, in terms of both the relative feature strengths and positions (Hudgins, Sandford, & Allamandola 1994; Hudgins & Allamandola 1995a, 1995b, 1997, 1998; Szczepanski & Vala 1993a, 1993b; Szczepanski, Chappo, & Vala 1993; Szczepanski et al. 1995a, 1995b).

Here we make a detailed comparison between recently available laboratory data and spatial and spectral variations in the infrared spectrum from the SVS 3 region in the

reflection nebula NGC 1333. SVS 3 is an early B star (Strom, Vrba, & Strom 1976; Harvey, Wilking, & Joy 1984), producing a much milder UV spectrum than found in other PAH emission regions (e.g. the Orion Bar, NGC 7027). Joblin et al. (1996) obtained discrete mid-infrared spectra in 3 locations in the reflection nebula using a $5''$ beam and found that the strength of the 8.6 and $11.2\ \mu\text{m}$ PAH features varied inversely to each other, with the $8.6\ \mu\text{m}$ feature emitting more strongly near SVS 3 and the $11.2\ \mu\text{m}$ feature emitting more strongly to the south away from SVS 3. Since the $8.6\ \mu\text{m}$ feature shows enhanced strength in the spectra of most PAH cations (along with the other bands between 6 and $10\ \mu\text{m}$), Joblin et al. concluded that SVS 3 was ionizing a larger fraction of the PAHs closer in than further away. This dependence of ionization fraction as a function of distance from the ionizing source could easily result from geometric dilution.

This investigation concentrates on emission features in the $10\text{--}13\ \mu\text{m}$ spectral region, which arise from out-of-plane bends of C–H bonds on the periphery of PAH molecules (e.g. Bellamy 1958; Allamandola, Tielens, & Barker 1989). For *neutral* PAHs the strongest feature at $11.2\ \mu\text{m}$ originates in PAH rings which contain only one C–H bond (the solo mode). The duo mode (two adjacent C–H bonds) produces a feature in the vicinity of $11.9\ \mu\text{m}$, but this feature is much weaker in astronomical sources. Since in the laboratory spectra of PAHs the wavelength of these bands can shift a substantial fraction of a micron, depending on the size and structure of the molecule, the positions of the solo and duo modes have long been used by chemists as a diagnostic of PAH structure. The trio mode produces a feature at $\sim 13\ \mu\text{m}$, but the wavelength range of this mode overlaps with the quartet and quintet modes at longer wavelengths, making unambiguous identification difficult.

2. Observations and analysis

In order to investigate the spectral variations in the PAH emission at higher spatial resolution, we obtained long-slit 8–13 μm spectra of NGC 1333 SVS 3 at the 5-m Hale Telescope at Palomar on the nights of 1996 September 29–30 (UT) using SpectroCam-10 (Hayward et al. 1993).¹ The data have a spectral resolution of 0.19 μm and a diffraction-limited angular resolution of $\sim 0''.5$. The slit was oriented N/S and covered a $2 \times 16''$ region of the sky including SVS 3 and the nebulosity to the south. We used standard chop-and-nod sequences with 40'' and 60'' amplitudes E/W to correct for background emission from the telescope and sky. The data were flux-calibrated using spectra of β Peg taken immediately before or after the NGC 1333 observations, together with archival SpectroCam-10 ratio spectra of β Peg vs. α Lyr and the absolute α Lyr model from Cohen et al. (1992). The data from the two nights were combined into a single 2-D spectral image from which individual 1-D spectra were extracted for plotting.

Figure 1 illustrates the spectrum summed from 2'' south of SVS 3 to the end of the slit, showing the 8.6 μm feature on the shoulder of the stronger 7.7 μm feature, the 11.2 μm feature and the emission plateau extending to the weaker 12.7 μm feature. Figure 2 shows how the strengths of the PAH features vary with position along the slit. While the 11.2 and 12.7 μm features grow progressively stronger toward the PAH emission ridge 10'' south of SVS 3, the 8.6 μm feature is stronger closer in. This behavior confirms the results of Joblin et al. (1996).

Fig. 3 shows how the shape of the 11.2 μm feature (solo mode) changes as a function of

¹Observations at Palomar Observatory were made as part of a continuing collaborative agreement between the California Institute of Technology, Cornell University, and the Jet Propulsion Laboratory.

distance from SVS 3. Close to the source, the feature has an excess on the short-wavelength wing, which appears to consist of multiple components. As the distance from SVS 3 increases, the shorter wavelength portion of the wing (centered at $\sim 10.8 \mu\text{m}$) disappears first, followed by the longer wavelength portion (at $\sim 11.0 \mu\text{m}$).

We have extracted the flux from these two components (Fig. 4), which we describe as the “blue outliers” to the $11.2 \mu\text{m}$ feature, by averaging the profile of the $11.2 \mu\text{m}$ feature $8''$ south of SVS 3 (and beyond), normalizing this mean profile to each row, and subtracting it. The $10.8 \mu\text{m}$ outlier is summed from 10.6 to $10.9 \mu\text{m}$ and the $11.0 \mu\text{m}$ outlier is summed from 10.9 to $11.2 \mu\text{m}$. While the $10.8 \mu\text{m}$ outlier goes to zero $8''$ from SVS 3, the $11.0 \mu\text{m}$ outlier still makes a contribution, which we crudely estimate to be $0.91 \times 10^{-16} \text{ W m}^{-2} \text{ arcsec}^{-2}$ at this position by fitting a gaussian to the blue edge of the main band at $11.2 \mu\text{m}$. Both outliers increase in strength by a factor of ~ 2 close to SVS 3 despite the fact that the stronger features at 8.6 , 11.2 , and $12.7 \mu\text{m}$ are at a minimum in this region (Fig. 2).

Our observations of NGC 1333 suggest that the $12.7 \mu\text{m}$ feature also develops a blue wing close to the central source. Because of the poor signal-to-noise in this spectral region, deep atmospheric absorption features (due to water vapor at 12.38 , 12.44 , 12.52 , and $12.56 \mu\text{m}$ and CO_2 at $12.63 \mu\text{m}$), and the complications introduced by possible $[\text{Ne II}]$ emission at $12.78 \mu\text{m}$, we cannot be more conclusive or quantitative with the present data.

An emission feature in the vicinity of $9.8 \mu\text{m}$ also appears within $1''$ of SVS 3 (Fig. 5). This feature occurs on the wing of a very strong telluric absorption feature from O_3 , making its apparent wavelength dependent on the quality of the atmospheric correction and difficult to determine accurately. However, the feature in our spectrum cannot arise entirely from a poor telluric correction, or it would appear along the entire length of the slit and not just near SVS 3. The $10 \mu\text{m}$ feature also appears in the on-source spectrum of SVS 3 by Joblin et al. (1996), but without comment and only at the $1\text{-}\sigma$ level. The feature has

also appeared (faintly, and without comment) in spectra obtained from the Infrared Space Observatory (Beintema et al. 1996) and the Infrared Telescope in Space (Yamamura et al. 1996). Both of these telescopes are above all atmospheric ozone. This feature probably does not arise from silicate dust, because silicates would produce a much broader emission band.

3. Discussion

A component in the vicinity of $11.0\ \mu\text{m}$ has appeared before in the spectra of several PAH sources, most strongly in TY CrA (at $\sim 11.05\ \mu\text{m}$; Roche, Aitken, & Smith 1991), but also in Elias 1 (at $\sim 11.06\ \mu\text{m}$; Hanner, Brooke, & Tokunaga 1994), and more weakly in several other sources, including Elias 14 (at $\sim 10.8\ \mu\text{m}$; Hanner, Brooke, & Tokunaga 1995) and WL 16 (DeVito & Hayward 1998). The WL 16 data (also obtained with SpectroCam-10 at Palomar) show spatial behavior similar to our NGC 1333 data, with the blue wing on the $11.2\ \mu\text{m}$ feature becoming more pronounced closer to the central source and fading further away (Fig. 3 in DeVito & Hayward 1998).

To determine the nature of the blue outliers and the $10\ \mu\text{m}$ feature, we compare our astronomical data to the database of spectra from the Astrochemistry Laboratory Group at NASA Ames Research Center (Hudgins et al. 1994; Hudgins and Allamandola 1995a, 1995b, 1997, 1998) and theoretical models by Langhoff (1996).

For neutral PAHs, Langhoff (1996) finds that the position of the $11.2\ \mu\text{m}$ feature depends on the geometry of the molecule. Moving from a small molecule like anthracene (three adjacent rings) to tetracene (four rings) to pentacene (five rings), the feature shifts from 11.3 to $10.9\ \mu\text{m}$. This shift raises the possibility that the blue outliers might result from a change in the composition of the PAH mixture. However, the laboratory data of Hudgins et al. show a much smaller shift in wavelength as a function of molecular size.

From anthracene to pentacene, the feature only shifts from 11.3 to 11.1 μm .

The relative strengths of the 11.2 and 12.7 μm bands provide a crude means of probing the size of the PAHs. In larger PAHs, the solo mode (11.2 μm) would dominate, since any ring along a straight edge of the molecule would have only one C–H bond, while the trio mode (12.7 μm) would appear more frequently in smaller PAHs, where a larger fraction of the rings occupy corners and not straight edges. As Fig. 2 shows, the spatial behaviors of both the 11.2 and 12.7 μm features agree with each other within the uncertainties, pointing to closely related sets of carriers and not variations in the size of the PAHs. Consequently, we do not consider it likely that the blue outliers to the 11.2 μm feature result from changes in the size distribution or molecular geometry of the PAHs sampled by the slit.

Figures 6 and 7 compare the laboratory and theoretical spectra of neutral PAHs and PAH cations. In the cations, most of the C–H out-of-plane bending modes have shifted $\sim 0.4 \mu\text{m}$ to shorter wavelengths (Fig. 6), providing a straightforward interpretation of the blue outliers seen close to SVS 3. Figure 7 shows that the 10 μm feature seen near SVS 3 may also arise from PAH cations, since PAH cations consistently produce features in this wavelength region while neutral PAHs do not.

Joblin et al. (1996) argued that the fraction of PAH cations decreases further from SVS 3 due to decreasing fluxes of ionizing photons. In our data, the blue outliers to the 11.2 μm feature and the 10 μm feature show just this spatial dependence. The combination of this spatial behavior and the appearance of similar spectral features in laboratory spectra of ionized PAHs leads us to identify these features with PAH cations.

This identification substantially strengthens the case for PAHs as carriers of the UIR bands. The identification of the 3.29 μm band with the aromatic C–H stretch and the bands in the 11–13 μm region with out-of-plane C–H bends requires that the carrier consist of aromatic hydrocarbons, but the nature of these aromatic hydrocarbon molecules

has remained in doubt (e.g. Sellgren 1994, Tokunaga 1997, Uchida et al. 1998). Energy requirements discussed in the proposal of PAHs as possible carriers of the UIR bands (Leger & Puget 1984; Allamandola et al. 1985) lead to estimates that these molecules must contain $\sim 40\text{--}80$ carbon atoms. Therefore, they must be polycyclic. But these molecules might exist within a larger matrix of hydrocarbons and other molecules, commonly described as hydrogenated amorphous carbon (HAC; see the recent review by Duley 1993). In order for the molecules to be ionized, they *must be free molecules*, i.e. they must be separate from any HAC-like matrix. In the face of these combined arguments, individual gas-phase PAHs must be the dominant emitters of the narrow UIR bands.

The authors thank Walt Duley and Craig Smith for helpful discussions. We would also like to express our gratitude to an anonymous referee who returned comments to us in only two weeks. During the preparation of this manuscript, GCS was supported by NSF grant INT-9703665 and graciously hosted by the School of Physics, Australian Defence Force Academy, and the Division of Physics and Electronics Engineering, University of New England.

REFERENCES

- Allamandola, L.J. 1996, in *The Cosmic Dust Connection*, ed. J.M. Greenberg, (Dordrecht: Kluwer), 81
- Allamandola, L.J., Tielens, A.G.G.M., & Barker, J.R. 1985, *ApJ*, 290, L25
- Allamandola, L.J., Tielens, A.G.G.M., & Barker, J.R. 1989, *ApJS*, 71, 733
- Beintema, D.A., Van den Ancker, M.E., Molster, F.J., Waters, L.B.F.M., Tielens, A.G.G.M., Waelkens, C., De Jong, T., De Graauw, T., Justannont, K., Yamamura, I., Heras, A., Lahuis, F., & Salama, A. 1996, *A&A*, 315, 369
- Bellamy, L.J. 1958, *The Infra-red Spectra of Complex Molecules* (2nd Ed., New York: Wiley) 65
- Cohen, M., Walker, R. G., Barlow, M. J., & Deacon, J. R. 1992, *AJ*, 104, 1650
- DeVito, B., & Hayward, T.L. 1998, *ApJ*, 504, 43
- Duley, W.W. 1993, in *Dust and Chemistry in Astronomy*, ed. T.J. Millar and D.A. Williams, (Bristol: Institute of Physics Publishing), 71
- Gillett, F.C., Forrest, W.J., & Merrill, K.M. 1973, *ApJ*, 183, 87
- Harvey, P.M., Wilking, B.A. & Joy, M. 1984, *ApJ*, 278, 156
- Hayward, T.L., Miles, J.W., Houck, J.R., Gull, G.E., & Schoenwald, J. 1993, *Proc. SPIE*, 1946, 334
- Hanner, M.S., Brooke, T.Y., & Tokunaga, A.T. 1994, *ApJ*, 433, L97
- Hanner, M.S., Brooke, T.Y., & Tokunaga, A.T. 1995, *ApJ*, 438, 250
- Hudgins, D.M., Sandford, S.A., & Allamandola, L.J. 1994, *JPC*, 98, 4243
- Hudgins, D.M., & Allamandola, L.J. 1995a, *JPC*, 99, 3033
- Hudgins, D.M., & Allamandola, L.J. 1995b, *JPC*, 99, 8978

- Hudgins, D.M., & Allamandola, L.J. 1997, JPC, 101, 3472
- Hudgins, D.M., & Allamandola, L.J. 1998, in preparation
- Joblin, C., Tielens, A.G.G.M., Geballe, T.R., & Wooden, D.H. 1996, ApJ, 460, L119
- Langhoff, S.R. 1996, JPC, 100, 2819
- Leger, A., & Puget, J.L. 1984, A&A, 137, L5
- Roche, P.F., Aitken, D.K., & Smith, C.H. 1991, MNRAS, 252, 282
- Sellgren, K. 1994, in The First Symposium on the Infrared Cirrus and Diffuse Interstellar Clouds, ed. R.M. Cutri and W.B. Latter, 243
- Strom, S.E., Vrba, F.J., & Strom, K.M. 1976, AJ, 81, 314
- Szczepanski, J., Chapo, C., & Vala, M. 1993, Chem Phys Letters, 205, 434
- Szczepanski, J. & Vala, M. 1993a, Nature, 363, 699
- Szczepanski, J. & Vala, M. 1993b, ApJ, 414, 646
- Szczepanski, J., Wehlburg, C. & Vala, M. 1995, Chem Phys Letters, 232, 221
- Szczepanski, J., Drawdy, J., Wehlburg, C. & Vala, M. 1995, Chem Phys Letters, 245, 539
- Tokunaga, A. 1997, in Diffuse Infrared Radiation and the IRTS, ed. H. Okuda, T. Matsumoto, & T. Roellig, ASP Conf. Series, Vol. 124, 149
- Uchida, K.I., Sellgren, K., & Werner, M. 1998, ApJ, 493, 109
- Yamamura, I., Onaka, T., Tanabe, T., Roellig, T.L., & Yuen, L. 1996, PASJ, 48, L65

Fig. 1.— The average spectrum from the PAH emission region south of SVS 3, determined from $2''$ away from SVS 3 to the south end of the spectrometer slit. The error bars represent $1\text{-}\sigma$ uncertainties.

Fig. 2.— Equivalent fluxes from the PAH features at $8.6\text{ }\mu\text{m}$ (*top*), $11.2\text{ }\mu\text{m}$ (*middle*), and $12.7\text{ }\mu\text{m}$ (*bottom*), determined by fitting and subtracting a linear baseline from beneath each feature. The $11.2\text{ }\mu\text{m}$ spatial profile (*dashed line*) has been normalized and plotted (*top and bottom*) for comparison.

Fig. 3.— Normalized spectral profiles of the $11.2\text{ }\mu\text{m}$ feature after removing a linear baseline, color-coded by position. The lengths of the vertical bars above the profiles illustrate the average $1\text{-}\sigma$ uncertainty in the data for each spectral strip. These strips are $1''.5$ wide.

Fig. 4.— The strength of the blue outliers of the $11.2\text{ }\mu\text{m}$ feature as a function of position in the slit, determined by fitting and subtracting the mean $11.2\text{ }\mu\text{m}$ feature $8''$ south of SVS 3 and beyond. The $10.8\text{ }\mu\text{m}$ outlier (summed from 10.6 to $10.9\text{ }\mu\text{m}$) is plotted with *squares*) and the $11.0\text{ }\mu\text{m}$ outlier ($10.9\text{--}11.2\text{ }\mu\text{m}$) is plotted with *circles*. We estimate that the $11.0\text{ }\mu\text{m}$ outlier still contributes $0.9 \times 10^{-16}\text{ W m}^{-2}\text{ arcsec}^{-2}$ at $8''$ from SVS 3.

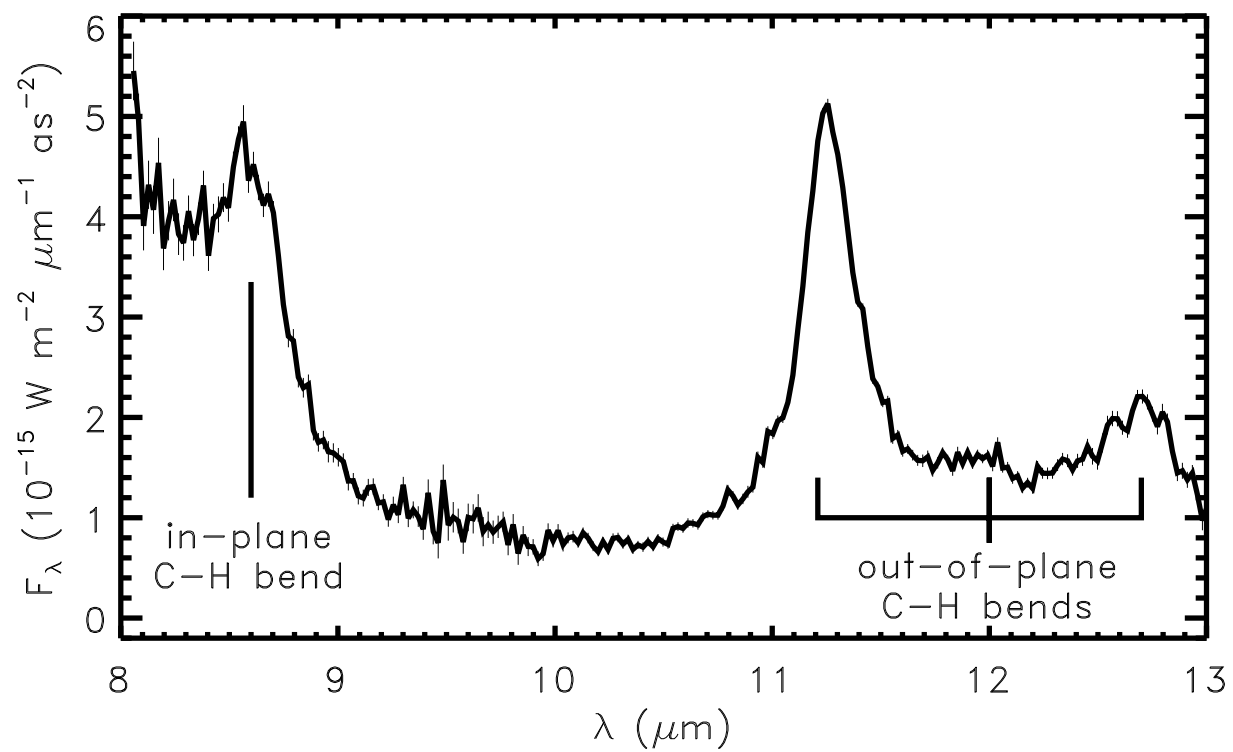
Fig. 5.— The spatial behavior of the spectrum at $10\text{ }\mu\text{m}$ in $1''$ steps, after removing a linear baseline. The black error bars show how the uncertainties vary with wavelength over this spectral range, primarily as a result of absorption from ozone in Earth’s atmosphere at $9.6\text{ }\mu\text{m}$. These data have been smoothed in both the spectral and spatial directions.

Fig. 6.— Laboratory and theoretical spectra for comparison with Fig. 3, produced by generating gaussian profiles from the wavelengths and strengths published by Hudgins et al. (1994), Hudgins and Allamandola (1995a, 1995b, 1997) and Langhoff (1996). The spectra are the sum of anthracene, tetracene, and chrysene (chosen because these molecules produce emission features in the vicinity of $11.2\text{ }\mu\text{m}$).

Fig. 7.— Laboratory and theoretical spectra for comparison to Fig. 5, generated as in Fig. 6, except that all molecules with both neutral and cation spectra in each set have been summed.

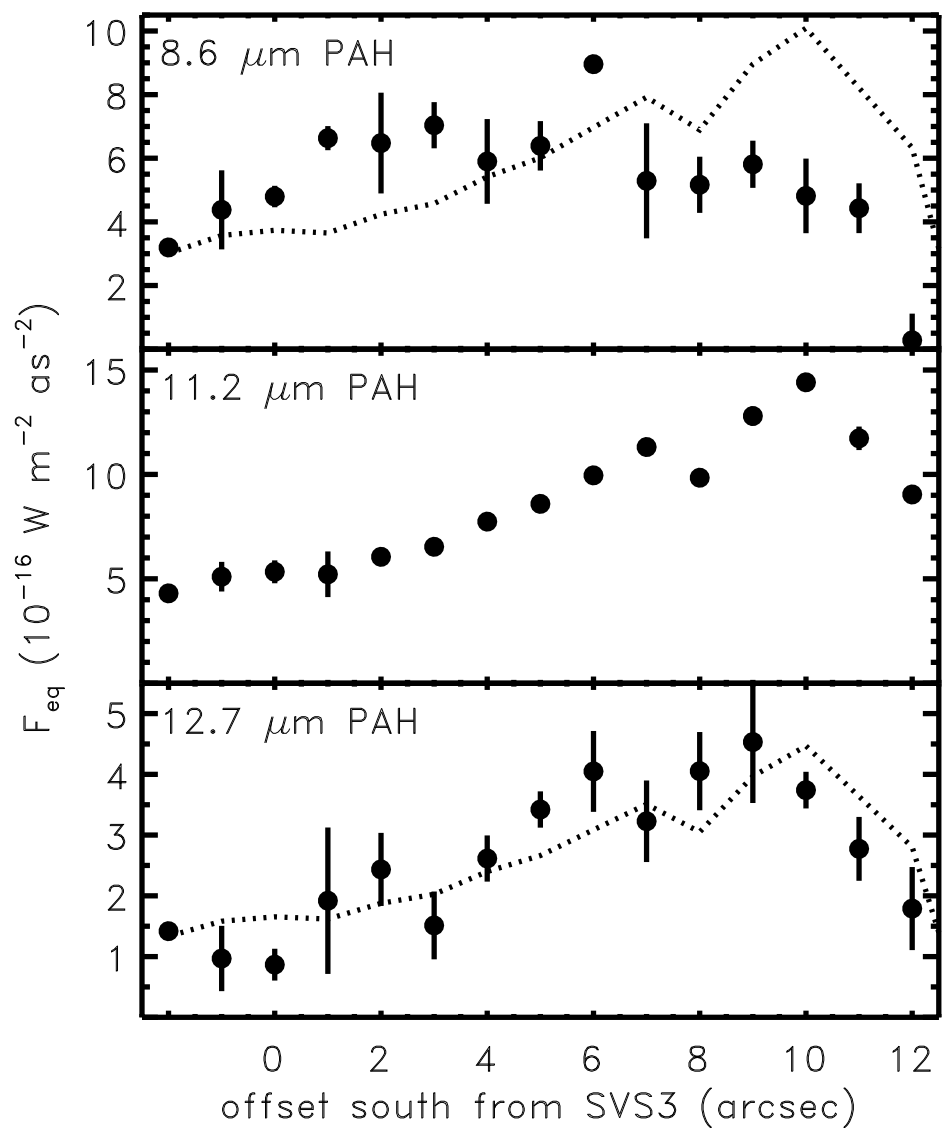
This figure "fig1.gif" is available in "gif" format from:

<http://arxiv.org/ps/astro-ph/9902077v1>



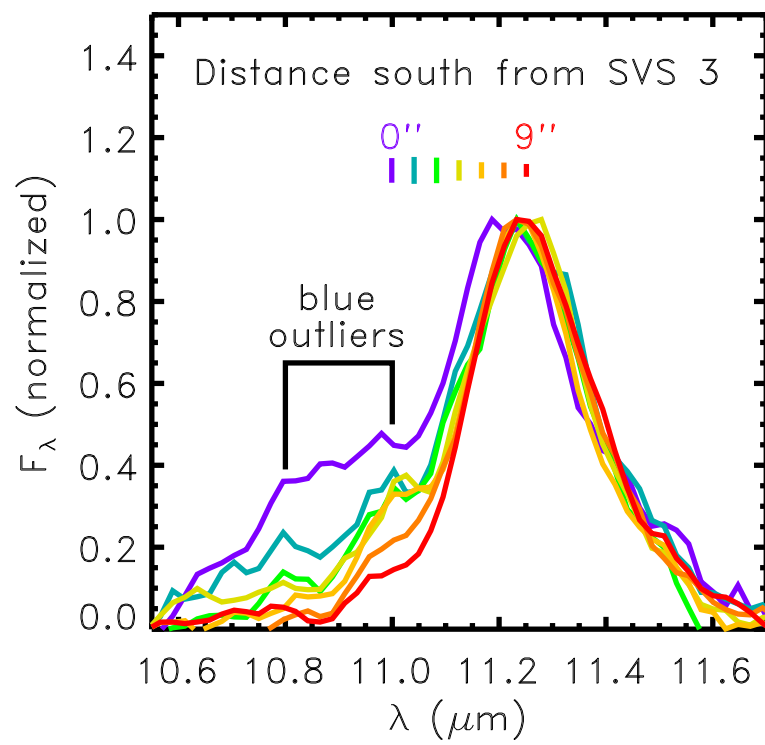
This figure "fig2.gif" is available in "gif" format from:

<http://arxiv.org/ps/astro-ph/9902077v1>



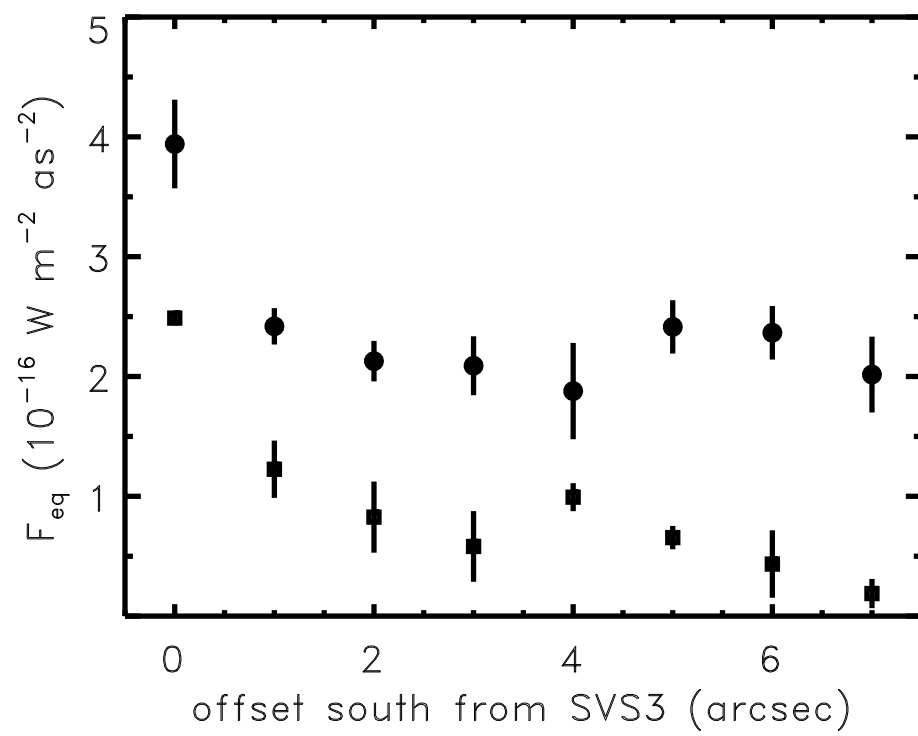
This figure "fig3.gif" is available in "gif" format from:

<http://arxiv.org/ps/astro-ph/9902077v1>



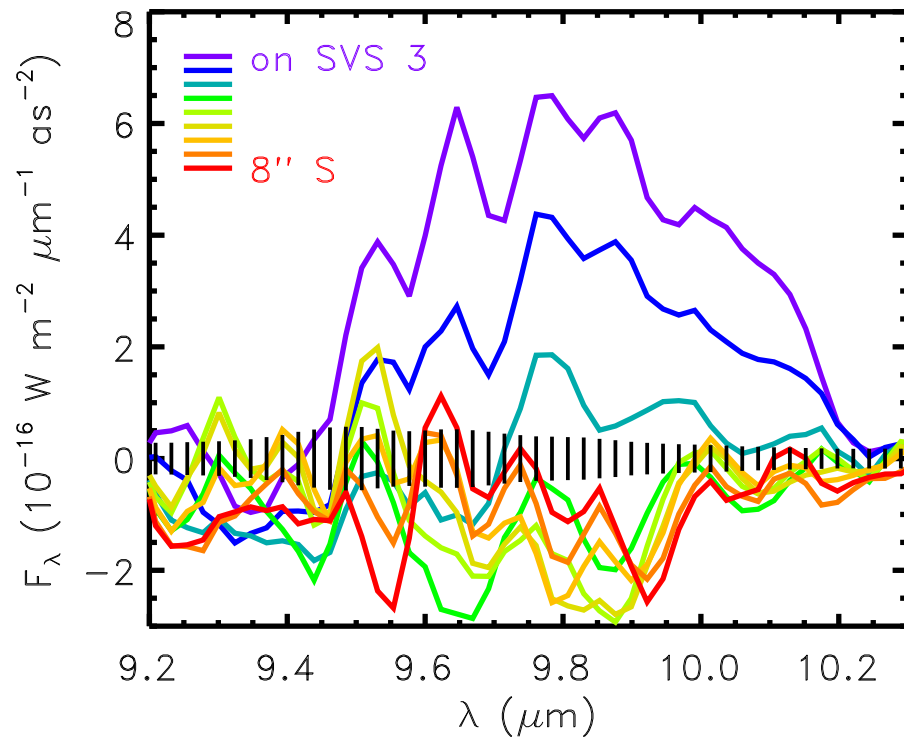
This figure "fig4.gif" is available in "gif" format from:

<http://arxiv.org/ps/astro-ph/9902077v1>



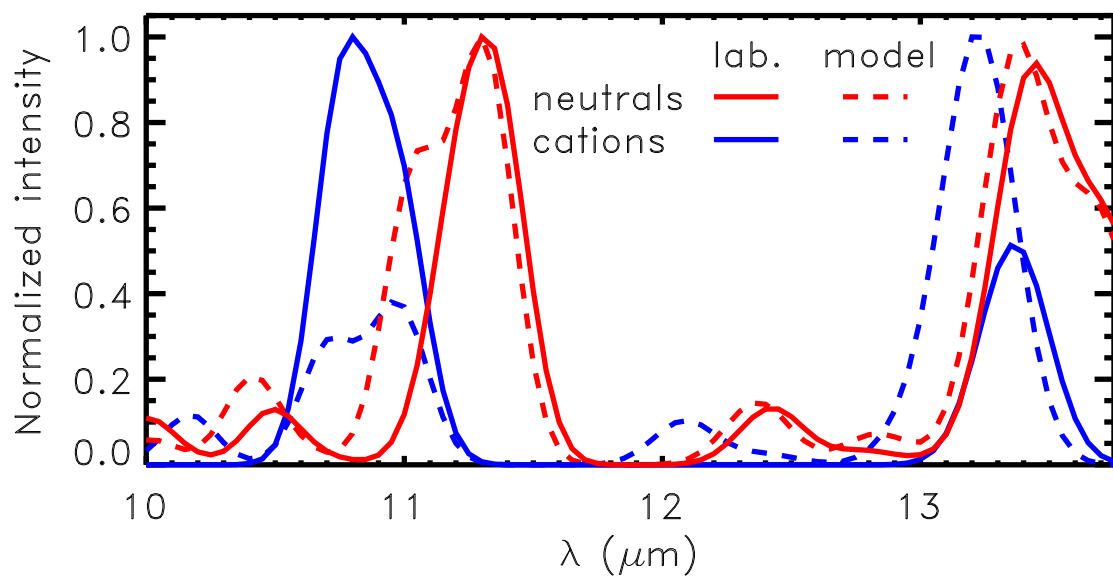
This figure "fig5.gif" is available in "gif" format from:

<http://arxiv.org/ps/astro-ph/9902077v1>



This figure "fig6.gif" is available in "gif" format from:

<http://arxiv.org/ps/astro-ph/9902077v1>



This figure "fig7.gif" is available in "gif" format from:

<http://arxiv.org/ps/astro-ph/9902077v1>

